PHYSICAL REVIEW B **78**, 020502(R) (2008)

Quantum oscillations in the mixed state of *d*-wave superconductors

Ashot Melikyan[1] and Oskar Vafek[2]
[1]*Materials Science Division, Argonne National Laboratory, Argonne, Illinois 60439, USA*
[2]*National High Magnetic Field Laboratory and Department of Physics, Florida State University, Tallahassee, Florida 32306, USA*
(Received 27 May 2008; published 2 July 2008)

We show that the low-energy density of quasiparticle states in the mixed state of ultraclean $d_{x^2-y^2}$-wave superconductors exhibits quantum oscillations even in the regime where the cyclotron frequency $\hbar\omega_c \ll \Delta_0$, the *d*-wave pairing gap. Such oscillations as a function of magnetic field B are argued to be due to the internodal scattering of the nodal quasiparticles near wave vectors $(\pm k_D, \pm k_D)$ by the vortex lattice as well as their Zeeman coupling. While the nominal periodicity of the oscillations is set by the condition $k_D[hc/(eB)]^{1/2} \equiv k_D'[hc/(eB')]^{1/2} (\mathrm{mod}\, 2\pi)$, we find that there is additional structure within each period that grows in complexity as the Dirac node anisotropy increases.

DOI: 10.1103/PhysRevB.78.020502 PACS number(s): 74.25.Jb, 74.25.Ha, 74.25.Qt

The behavior of $d_{x^2-y^2}$-wave superconductors in magnetic field has recently come into sharp focus due to the experimental observation of the oscillations in the longitudinal and Hall electrical transport, as well as magnetization, at extremely high magnetic fields for very clean underdoped $YBa_2Cu_3O_{6.5}$ (Ref. 1) and $YBa_2Cu_4O_8$.[2,3] At temperatures about 2 K and for magnetic fields in excess of about 30 T, the Hall resistance is finite, *negative* (i.e., electron like), and oscillates as a function of magnetic field, with approximately four pronounced peaks between ~45 and 60 T. Below about 30 T, the system is in the mixed superconducting state, and the electrical Hall conductivity vanishes. The current interpretation of these oscillations involves charge- or spin-order-induced reconstruction of the Fermi surface with electron pockets,[1,3–6] which result from the appropriate tuning of the strength of the charge or spin potentials in the particle-hole channel.[4–6]

As the estimated mean field H_{c2} for the YBCO samples in question significantly exceeds 60 T,[7] it is at present unclear why one should expect the superconducting order parameter amplitude to collapse at the fields applied in Refs. 1–3. Instead, the local superconducting correlations should persist, and rather the system is expected to be in the vortex liquid state.[8–10] Additionally, the sign reversal of the Hall effect, from positive to negative, with decreasing temperature near T_c in optimally doped YBCO has been observed and interpreted earlier as resulting from the flux flow.[11–13] The structure factor of such a liquid state is expected to closely resemble that of a vortex solid. In this context, the natural question is the existence, the periodicity, and the physical nature of such magnetic-field-induced oscillations in the vortex state.

In this work, we therefore examine the properties of the *d*-wave quasiparticles (qps) in the vortex solid state at intermediate magnetic fields, i.e., we examine the particle-particle channel. For the square vortex lattice observed in the small-angle neutron scattering,[14] we find that the combined effect of the orbital and spin coupling of the qps to the magnetic field does induce oscillations in the low-energy density of states (DOS), $N(E)$, and that the nature of these oscillations depends on the Dirac cone anisotropy α_D. In the physically relevant regime where the *d*-wave gap $\Delta_0 \gg \hbar\omega_c$ (the cyclotron frequency $\omega_c = eB/mc$), the density of states $N(E)$ is an oscillatory function of $k_D\ell$, where k_D is the k-space half-distance between the nearest nodes (see Fig. 1) and ℓ is the magnetic length $\ell = \sqrt{hc/Be}$. For $\alpha_D = 1$, the period of the oscillations corresponds to $\delta(k_D\ell) = 2\pi$, but with increasing anisotropy the number of oscillations *within* the period increases. In the absence of Zeeman coupling, $N(E)$ is exactly periodic in the scaling regime and the spectrum oscillates between fully gapped and nodal. Upon inclusion of the Zeeman coupling, which cannot be neglected for fields of Refs. 1–3, the oscillatory behavior persists, but the scaling is only approximate. For $\alpha_D = 1$ and for fields above 30 T, the combined effect of the orbital and Zeeman coupling leads to a sequence of transitions and the system oscillates between a thermal metal with finite $N(0)$ and a thermal insulator with vanishing $N(0)$. A similar pattern of oscillating behavior holds for large α_D, albeit with effectively increased frequency and significantly decreased gap. The envelope of the $N(0)$ oscillations follows an approximately ℓ^{-1} behavior. These findings should be contrasted with the oscillations found in the regime of extreme high fields reviewed in Ref. 15 and, for *d*-wave superconductors, with Ref. 16, where the number of Landau levels below the Fermi energy ranges from 1 to 7.

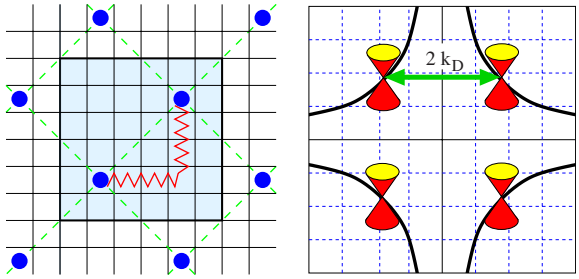

FIG. 1. (Color online) Left: Magnetic unit cell $\ell \times \ell$ of a tight-binging lattice (solid lines) containing two vortices joined by a branch cut shown for $\ell = 6a$. Right: Fermi surface (black solid lines) with four nodal points at $\mathbf{k}_F^{(j)} = (\pm k_D, \pm k_D)$ in a Brillouin zone of size $2\pi/a$. In the presence of the vortex lattice, the Brillouin zone is reduced to $2\pi/\ell$ (spacing of the blue dashed grid). The properties of the low-energy states depend on the commensuration between the internodal distance $2k_D$ and $2\pi/\ell$.

The starting point is the lattice Bogoliubov–de Gennes (BdG) eigenvalue equation[17,18]

$$\hat{\mathcal{H}}_0\psi_{\mathbf{r}} = E\psi_{\mathbf{r}}, \tag{1}$$

where the Hamiltonian $\hat{\mathcal{H}}_0$ acts on the two-component Nambu spinor $\psi_{\mathbf{r}}=[u_{\mathbf{r}},v_{\mathbf{r}}]^T$ and has the following explicit form:

$$\hat{\mathcal{H}}_0 = \begin{pmatrix} \hat{\mathcal{E}}_{\mathbf{r}} - \mu + \frac{g}{2}\mu_B B & \hat{\Delta}_{\mathbf{r}} \\ \hat{\Delta}^*_{\mathbf{r}} & -\hat{\mathcal{E}}^*_{\mathbf{r}} + \mu + \frac{g}{2}\mu_B B \end{pmatrix}. \tag{2}$$

Both $\hat{\mathcal{E}}_{\mathbf{r}}$ and $\hat{\Delta}_{\mathbf{r}}$ are defined through their action on a lattice function $f_{\mathbf{r}}$ as

$$\hat{\mathcal{E}}_{\mathbf{r}} f_{\mathbf{r}} = -t \sum_{\delta=\pm\hat{\mathbf{x}},\pm\hat{\mathbf{y}}} e^{-i\mathbf{A}_{\mathbf{r}\mathbf{r}+\delta}} f_{\mathbf{r}+\delta}, \tag{3}$$

$$\hat{\Delta}_{\mathbf{r}} f_{\mathbf{r}} = \Delta_0 \sum_{\delta=\pm\hat{\mathbf{x}},\pm\hat{\mathbf{y}}} e^{i\theta_{\mathbf{r}\mathbf{r}+\delta}} \eta_\delta f_{\mathbf{r}+\delta}. \tag{4}$$

In the symmetric gauge, the magnetic flux Φ through an elementary plaquette enters the Peierls factor via $\mathbf{A}_{\mathbf{r}\mathbf{r}+\hat{x}} = -\pi y\Phi/\phi_0$, $\mathbf{A}_{\mathbf{r}\mathbf{r}+\hat{y}} = \pi x\Phi/\phi_0$; the electronic flux quantum is $\phi_0 = hc/e$. The d-wave symmetry is encoded in $\eta_\delta = +(-)$ if $\delta \| \hat{\mathbf{x}}(\hat{\mathbf{y}})$. Importantly, $\theta_{\mathbf{r}\mathbf{r}'}$ winds by 2π around each of the magnetic-field-induced vortices. The initial ansatz[19] for the pair phases is

$$e^{i\theta_{\mathbf{r}\mathbf{r}'}} \equiv (e^{i\phi_{\mathbf{r}}} + e^{i\phi_{\mathbf{r}'}})/\left|e^{i\phi_{\mathbf{r}}} + e^{i\phi_{\mathbf{r}'}}\right|, \tag{5}$$

where $\nabla\times\nabla\phi(\mathbf{r}) = 2\pi\hat{\mathbf{z}}\Sigma_i\delta(\mathbf{r}-\mathbf{r}_i)$ and $\nabla\cdot\nabla\phi(\mathbf{r}) = 0$, where $\mathbf{r}_i$ denotes the vortex positions. Although the phase of the order parameter does depend on the precise form of the self-consistency condition, the deviations from the adopted form are weak, and moreover, both the symmetry of the phase and its singular part are fixed unambiguously by the vortex lattice.

Connecting pairs of vortices by branch cuts,[19] we can define the singular gauge transformation[19,20] $\mathcal{U} = e^{(i/2)\sigma_3\phi_{\mathbf{r}}}$, where the Pauli sigma matrices act on the Nambu spinors. The transformed Hamiltonian $\mathcal{H}(\mathbf{k}) = e^{-i\mathbf{k}\cdot\mathbf{r}}\mathcal{U}^{-1}\hat{\mathcal{H}}_0\mathcal{U}e^{i\mathbf{k}\cdot\mathbf{r}}$ becomes

$$\mathcal{H}(\mathbf{k}) = \sigma_3[\tilde{\mathcal{E}}_{\mathbf{r}}(\mathbf{k}) - \mu] + \sigma_1\tilde{\Delta}_{\mathbf{r}}(\mathbf{k}) + \frac{g}{2}\mu_B B, \tag{6}$$

where the transformed lattice operators satisfy

$$\tilde{\mathcal{E}}_{\mathbf{r}}(\mathbf{k})\psi_{\mathbf{r}} = -t \sum_{\delta=\pm\hat{\mathbf{x}},\pm\hat{\mathbf{y}}} z_{2,\mathbf{r}\mathbf{r}+\delta} e^{i\sigma_3 V_{\mathbf{r}\mathbf{r}+\delta}} e^{i\mathbf{k}\cdot\delta}\psi_{\mathbf{r}+\delta}, \tag{7}$$

$$\tilde{\Delta}_{\mathbf{r}}(\mathbf{k})\psi_{\mathbf{r}} = \Delta_0 \sum_{\delta=\pm\hat{\mathbf{x}},\pm\hat{\mathbf{y}}} z_{2,\mathbf{r}\mathbf{r}+\delta}\eta_\delta e^{i\mathbf{k}\cdot\delta}\psi_{\mathbf{r}+\delta}. \tag{8}$$

The physical superfluid velocity enters via the factor

$$e^{iV_{\mathbf{r}\mathbf{r}'}} = e^{-i\mathbf{A}_{\mathbf{r}\mathbf{r}'}}(1 + e^{i(\phi_{\mathbf{r}'}-\phi_{\mathbf{r}})})/\left|1 + e^{i(\phi_{\mathbf{r}'}-\phi_{\mathbf{r}})}\right| \tag{9}$$

and represents the lattice analog of the semiclassical (Doppler) effect.[21] The Z_2 field $z_{2,\mathbf{r}\mathbf{r}'} = 1$ on each bond except the ones crossing the branch cut, where $z_{2,\mathbf{r}\mathbf{r}'} = -1$. Note that $V_{\mathbf{r}\mathbf{r}'}$ and our choice of the branch cuts are periodic with the primitive vectors $\mathbf{R}_1 = \ell\hat{x}$ and $\mathbf{R}_2 = \ell\hat{y}$ defining the magnetic unit cell. By the Bloch condition, $\mathcal{H}(\mathbf{k})$ acts on the periodic functions, and the crystal wave vector $\mathbf{k}$ varies continuously within the first Brillouin zone $2\pi/\ell \times 2\pi/\ell$.

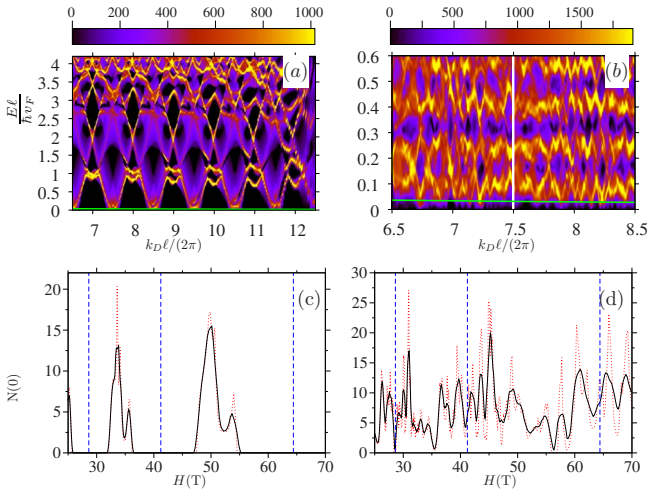

FIG. 2. (Color online) (a,b): Oscillations of the qp density of states $N(E)$ rescaled as $\ell v_F N[\ell E/(\hbar v_F)]$ are shown as a color map for $\alpha_D=1$ (a) and $\alpha_D=7$ (b). The nearly horizontal (green) line above zero represents the shift of the qp zero energy due to the Zeeman term for $t=380$ meV, $a=3.8$ Å, $g=2$, $k_D=0.38\pi/a$, and $\ell=26a$. (c,d) Zero-energy density of states of (2) as a function of magnetic field for $\alpha_\Delta=1$ (c) and 7 (d) deduced from the figures of the top row, and the generalized scaling form of eigenvalues (10) is shown by a red dashed line. The solid black line corresponds to an effective broadening due to the interlayer coupling $2t_z\cos(k_z c)$ with $t_z=0.05t$.

Since the Zeeman term is just a simple overall shift of the qp energies, let us first neglect it. The results of the numerical diagonalization of Eq. (6) can be summarized by the following scaling form of the qp energy eigenvalues:

$$E_n(\mathbf{k}) = \frac{\hbar v_F}{\ell}\mathcal{F}_n(\mathbf{k}\,\ell\,, \alpha_D, k_D\,\ell\,). \tag{10}$$

Here v_F and v_Δ are the Fermi and gap velocities of the d-wave qps near the nodes $(\pm k_D, \pm k_D)$ [in our model (2) $v_F = 2\sqrt{2}at\hbar^{-1}\sin(k_D a)$ and $v_\Delta = v_F\Delta_0/t$]; $\mathcal{F}_n$ is a dimensionless scaling function, which *differs* from the Simon-Lee scaling function in the following important aspect: *it depends on* $k_D\ell$. Specifically, when $k_D\ell\to\infty$, the function $\mathcal{F}_n$ does not approach a uniform value. This is amply illustrated in Fig. 2, where we used a color density plot to represent the DOS per area rescaled as $v_F\ell N(E)$ for different values of $k_D\ell/(2\pi)$ and $E\ell/(\hbar v_F)$.

As best seen for $\alpha_D=1$, near $E=0$ the spectrum is gapped although for $k_D\ell \approx \pi(2n+1)$ the gap is very small, vanishing only at a discrete set of points as expected for the unitary class.[18] Moreover, the gap scales as ℓ^{-1} and oscillates as a function of $k_D\ell$. Physically, the oscillations are due to the strong internodal scattering that arises from the commensurability of the d-wave nodes and the vortex lattice. As seen

from the two different panels, the pattern of oscillations depends on the anisotropy α_D. With increasing α_D, the DOS acquires ever richer structure with multiple minima and maxima—for presentation purposes, we show only two periods for $\alpha_D=7$. Additionally, as α_D increases, the scaling limit $\Delta_0 \gg \hbar\omega_c$ is reached for smaller magnetic fields (larger ℓ) and the approximate low-energy scaling (10) holds for magnetic length $\ell/a \gg \sqrt{4\pi\alpha_D}$.

The magnetic fields of experimental interest (45–70 T) correspond to $\ell \in (20a, 25a)$, which is the regime where the Zeeman term cannot be neglected. Nevertheless, it is easy to take it into account, since it corresponds to a simple shift in zero of the qp energy, represented by the green lines in each of the color DOS maps in Fig. 2. The DOS along the Zeeman "slice" is shown in Figs. 2(e) and 2(f). For anisotropy $\alpha_D=1$, the spectrum exhibits pronounced oscillations as a function of magnetic field (or k_D), changing from gapped (thermal insulator) with activated temperature dependence of the specific heat to gapless (thermal metal) with T-linear specific heat. This $\delta\ell = 2\pi/k_D$ periodic sequence of transitions between thermal metal and thermal insulator is significantly richer for $\alpha_D > 1$. Within each such "primitive" period, a complex structure develops, and the number of minima and maxima depends on α_D. For completeness, we include the effects of additional interlayer hopping terms $2t_z \cos(k_z c)$ present in real materials, where $t_z/t = 5-10\,\%$, which lead to an effective averaging of the DOS over $k_D\ell$ (see Fig. 2). For $\alpha_D=7$ and $k_D = 0.38\pi/a$, which are approximately[22] the physical values expected for the YBCO samples of Ref. 1, there are four "oscillations" in the field range ~45–60 T. Remarkably, this is precisely the experimentally observed "periodicity."[1]

Note that the effect described here occurs deep in the vortex state with a fully developed superconducting amplitude and does not rely on semiclassical orbits around electron pockets. Rather, as we now argue, it is a consequence of the commensuration involving the vortex lattice and the internodal separation (see Fig. 1). In the scaling regime of interest, $\Delta_0 \gg \hbar\omega_c$, the appropriate starting point should be the linearized approximation[20,23] of BdG Hamiltonian (6). In this approach, the low-energy qps with $E \ll \Delta_0$ are independent and behave as massless Dirac fermions interacting with vortices via the Doppler shift originating from the superflow $\mathbf{v}(\mathbf{r}) = \frac{\hbar}{2}\nabla\phi - \frac{e}{c}\mathbf{A}$. Additionally, the wave functions contain branch cuts connecting vortices pairwise.[18–20,23–26] The effective Hamiltonian[20,23–25] is then

$$\mathcal{H}_{\rm lin}/v_F = \frac{p_x+p_y}{\sqrt{2}}\sigma_3 + \alpha_D\frac{p_y-p_x}{\sqrt{2}}\sigma_1 + m\frac{v_x+v_y}{\sqrt{2}}. \quad (11)$$

In this approximation, $\mathcal{H}_{\rm lin}$ exhibits the Simon-Lee[23] scaling $\mathcal{H}_{\rm lin}(\mathbf{r}, v_F, v_\Delta) = \frac{\hbar v_F}{\ell}\mathcal{H}_{\rm lin}(\mathbf{r}/\ell, \alpha_D, 1)$ and the qp spectrum has a scaling form $E_n(\mathbf{k}) = \frac{\hbar v_F}{\ell}\mathcal{F}_n^{(\rm lin)}(\mathbf{k}\ell, \alpha_D)$.

Now, we consider the corrections due to the terms left out during linearization. Provided that $\mathbf{r}$ is not in the immediate vicinity of a vortex core ($r \gtrsim \xi$), the leading nonlinear corrections, such as $m\mathbf{v}^2(\mathbf{r})/2$, are typically omitted on the basis that they are smaller than the terms retained in Eq. (11) by a factor of $(k_D\ell)^{-1}$, which is small for typical fields of interest. However, such an estimate is incorrect. The effect of the nonlinear terms is amplified[26] by anomalously large (low-energy) qp wave functions, growing as $r^{-1/2}$ near vortex locations.[18,27] This divergence is eventually cut off only at $r \approx \xi$. A typical "perturbation," such as $m\mathbf{v}^2(\mathbf{r})$, results in the following matrix element between two eigenstates of $\mathcal{H}_{\rm lin}$ at nodes j and j': $I = \langle \Psi_{n\mathbf{k}}^{(j)} | m\mathbf{v}^2(\mathbf{r}) | \Psi_{n'\mathbf{k}'}^{(j')} \rangle$. Due to Bloch symmetry of the wave functions Ψ, the Bloch momenta $\mathbf{k}_F^{(j)} + \mathbf{k}$ and $\mathbf{k}_F^{(j')} + \mathbf{k}'$ must differ by a reciprocal-lattice vector $\mathbf{G}$. Importantly, $|I| \propto \frac{\hbar v_F}{\ell}\frac{1}{k_D\xi}[C_1 + C_2\cos(\mathbf{R}\cdot\mathbf{G})]$, *which is of the same order as the terms retained in* Eq. (11). Here $\mathbf{R}$ is the primitive vortex lattice vector and the vortex core size ξ serves as the small-distance cutoff of the otherwise divergent integrals.[26] Coefficients $C_{1,2}$, in general, depend on $\mathbf{k}$ and $\mathbf{k}'$, but not on $\mathbf{k}_F^{(j)}$ or $\mathbf{k}_F^{(j')}$.

Thus, due to the $r^{-1/2}$ behavior of the low-energy wave functions near vortex cores, the matrix elements I, and the resulting corrections to the energies, scale with magnetic length precisely as the energies of Eq. (11), namely as $\sim\ell^{-1}$. The relative magnitude of the corrections due to the nonlinearities compared to Eq. (11) is determined by the magnitude of the parameter $(k_D\xi)^{-1}$ rather than $(k_D\ell)^{-1}$. In cuprate superconductors, the former is typically of $\mathcal{O}(1)$ since ξ is of the order of a few lattice spacings. Thus, if the parameters of the BdG Hamiltonian (6) such as μ or ℓ are varied, the resulting qp spectrum evolves in a manner not captured by Eq. (11).

Based on the above argument, for the square vortex lattice under consideration we expect the spectra for nodal momentum k_D (k_D') and magnetic length ℓ (ℓ') to be similar when

$$k_D\ell \equiv k_D'\ell' (\mathrm{mod}\, 2\pi). \quad (12)$$

Thus, the Simon-Lee scaling should be generalized to Eq. (10). In the regime where the scaling (10) holds, the oscillatory part of the dispersion is fully determined by the product $k_D\ell$, and therefore the dependence of the spectrum on the magnetic field can be determined from the changes in k_D.[26] Finally, for $\mu=0$ [i.e., $k_D = \pi/(2a)$], the characteristic oscillations found in this work can be proven rigorously without appealing to the perturbation theory.[19] In this case, when ignoring the Zeeman coupling, the qp spectrum is gapless when $k_D\ell/(2\pi)$ is a half-integer and gapped when it is an integer.

Next we discuss briefly the relation of our results to the quasiclassical approximation often employed in the study of qps in the vortex lattices.[21] Consider Fig. 3, where the ratio of the specific heat to the temperature is plotted as a function of temperature. For simplicity, we set $g=t_z=0$. For $3 < \alpha_D < 20$, C/T exhibits a similar pattern characterized by two energy scales, the first set by the oscillatory field-induced qp gap $E_1 \approx 3.5\hbar v_F/(\ell\alpha_D^2)$ and the second by the width of the lowest magnetic band $E_2 \approx 1.5\hbar v_F/(\ell\alpha_D)$. At $T \gtrsim E_2$, the quasiclassical description applies,[21] the low T extrapolation of which would predict $C/T \propto \sqrt{H}$. In the interval $E_1 \ll T \ll E_2$, the quasiclassical approximation breaks down, and C/T exhibits a peak due to an isolated lowest magnetic band, however the Simon-Lee scaling holds approximately. At yet lower temperatures $T \lesssim E_1$, in the extreme quantum

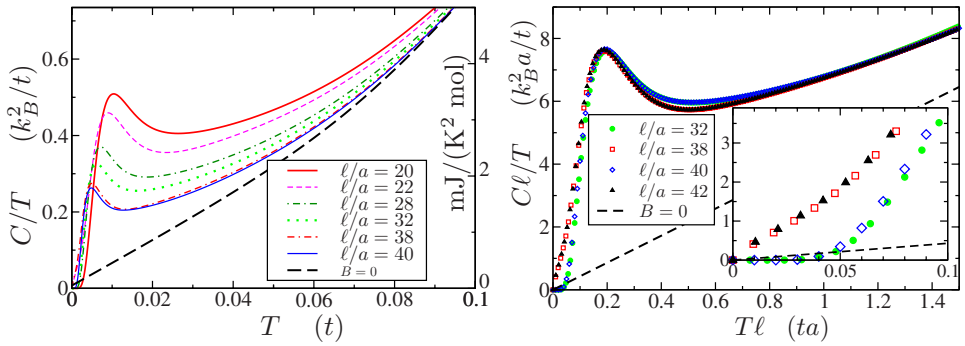

FIG. 3. (Color online) Left: C/T plotted as a function of T for $\alpha_D=5$, $\mu=0$, and different magnetic lengths ℓ/a. Right: same data on the scaling plot. Note the similarity of the cases $\ell/a=4n+2, n\in Z$ [i.e., $k_D\ell \equiv \pi(\mathrm{mod}\, 2\pi)$] at $T\ell \to 0$, and separately $\ell/a=4n$ [i.e., $k_D\ell \equiv 0(\mathrm{mod}\, 2\pi)$]. On the left vertical axis bars, C/T is per unit cell, per single CuO layer. C/T in physical units pertinent for YBCO is shown in the right vertical axis, using $v_F=2\sqrt{2}ta\approx 2.5\times 10^5$ m/s and $a=3.8$ Å.

regime, the specific heat exhibits pronounced oscillations as a function of the parameter $k_D\ell$, and the Simon-Lee scaling must be modified as in Eq. (10).

Since the effect described here is due to the interference effects between the nodal d-wave qps and the ordered vortex positions, it should be observable as long as the thermal length $\ell_T \sim \hbar v_\Delta/(k_B T)$ exceeds ℓ. We expect these oscillations to persist in a vortex liquid state with strong, albeit only short-range, positional order, provided that the vortex positional correlation length $\xi_p \gg \ell_T \gg \ell$. The true test of these predictions, however, would be an observation of the high-field quantum oscillations in the low-temperature specific heat in the superconducting state with a nearly perfect vortex lattice.

We thank Z. Tešanović for useful discussions. A.M. would also like to thank M. Norman for helpful discussions and a critical reading of the manuscript. A.M. was supported by the U.S. Department of Energy, Office of Science, under Contract No. DE-AC02-06CH11357. O.V was supported in part by the NSF Grant No. DMR-00-84173.

[1] N. Doiron-Leyraud, C. Proust, D. LeBoeuf, J. Levallois, J.-B. Bonnemaison, R. Liang, D. A. Bonn, W. N. Hardy, and L. Taillefer, Nature **447**, 565 (2007).
[2] E. A. Yelland, J. Singleton, C. H. Mielke, N. Harrison, F. F. Balakirev, B. Dabrowski, and J. R. Cooper, Phys. Rev. Lett. **100**, 047003 (2008).
[3] A. F. Bangura *et al.*, Phys. Rev. Lett. **100**, 047004 (2008).
[4] W.-Q. Chen, K.-Y. Yang, T. M. Rice, and F. C. Zhang, Europhys. Lett. **82**, 17004 (2008).
[5] A. J. Millis and M. R. Norman, Phys. Rev. B **76**, 220503(R) (2007).
[6] S. Chakravarty and H.-Y. Kee, arXiv:0710.0608 (unpublished).
[7] Y. Wang, N. P. Ong, Z. A. Xu, T. Kakeshita, S. Uchida, D. A. Bonn, R. Liang, and W. N. Hardy, Phys. Rev. Lett. **88**, 257003 (2002).
[8] D. R. Nelson and H. S. Seung, Phys. Rev. B **39**, 9153 (1989).
[9] D. A. Huse, M. P. A. Fisher, and D. S. Fisher, Nature **358**, 553 (1992).
[10] L. Li, J. G. Checkelsky, S. Komiya, Y. Ando, and N. P. Ong, Nat. Phys. **3**, 311 (2007).
[11] M. Galffy and E. Zirngiebl, Solid State Commun. **68**, 929 (1988).
[12] S. J. Hagen, C. J. Lobb, R. L. Greene, M. G. Forrester, and J. H. Kang, Phys. Rev. B **41**, 11630 (1990).
[13] T. R. Chien, T. W. Jing, N. P. Ong, and Z. Z. Wang, Phys. Rev. Lett. **66**, 3075 (1991); J. M. Harris, Y. F. Yan, O. K. C. Tsui, Y. Matsuda, and N. P. Ong, *ibid.* **73**, 1711 (1994).
[14] S. P. Brown, D. Charalambous, E. C. Jones, E. M. Forgan, P. G. Kealey, A. Erb, and J. Kohlbrecher, Phys. Rev. Lett. **92**, 067004 (2004).
[15] T. Maniv, V. Zhuravlev, I. Vagner, and P. Wyder, Rev. Mod. Phys. **73**, 867 (2001).
[16] K. Yasui and T. Kita, Phys. Rev. Lett. **83**, 4168 (1999); Phys. Rev. B **66**, 184516 (2002).
[17] Y. Wang and A. H. MacDonald, Phys. Rev. B **52**, R3876 (1995).
[18] O. Vafek, A. Melikyan, M. Franz, and Z. Tešanović, Phys. Rev. B **63**, 134509 (2001); O. Vafek, A. Melikyan, and Z. Tešanović, *ibid.* **64**, 224508 (2001).
[19] O. Vafek and A. Melikyan, Phys. Rev. Lett. **96**, 167005 (2006).
[20] M. Franz and Z. Tešanović, Phys. Rev. Lett. **84**, 554 (2000).
[21] G. E. Volovik, JETP Lett. **58**, 469 (1993).
[22] M. Sutherland *et al.*, Phys. Rev. B **67**, 174520 (2003).
[23] S. H. Simon and P. A. Lee, Phys. Rev. Lett. **78**, 1548 (1997).
[24] L. Marinelli, B. I. Halperin, and S. H. Simon, Phys. Rev. B **62**, 3488 (2000).
[25] A. Vishwanath, Phys. Rev. Lett. **87**, 217004 (2001); Phys. Rev. B **66**, 064504 (2002).
[26] A. Melikyan and Z. Tešanović, Phys. Rev. B **74**, 144501 (2006); Phys. Rev. B **76**, 094509 (2007).
[27] A. S. Mel'nikov, Phys. Rev. Lett. **86**, 4108 (2001).